ELSEVIER

Thermochimica Acta 395 (2003) 201–208

thermochimica acta

www.elsevier.com/locate/tca

New heat flux DSC measurement technique

Robert L. Danley*

TA Instruments, 109 Lukens Drive, New Castle, DE 19720, USA

Received 28 December 2001; accepted 16 March 2002

Abstract

The heat flow signal from a differential scanning calorimeter (DSC) includes significant artifacts related to the instrumentation. They may be categorized as those due to imbalances in the instrument or those resulting from instrument heat capacity effects, commonly known as "smearing". Imbalances cause instrument baseline defects that include offset, slope and curvature. Instrument heat capacity effects reduce the resolution of transitions and increase uncertainty when performing partial integrations of transitions. A new DSC heat flow measuring technique was developed that greatly reduces instrument baseline defects resulting from imbalances. It improves resolution and dynamic response by accounting for the instrument heat capacity effects. There are three components to the new heat flow measurement technique: (1) a new heat flow sensor assembly that has independent sample and reference calorimeters and incorporates two differential temperature measurements; (2) a more comprehensive heat flow measurement equation that includes calorimeter imbalances and differences in heating rates within the instrument and (3) a calorimetric calibration technique that characterizes the imbalances and enables the more comprehensive heat flow equation to be used. A DSC incorporating the new measurement displays a greatly improved instrument baseline and substantially improved resolution[1].

Keywords: DSC; Resolution; Baseline; Calibration; Sensor

1. Introduction

Among the more important performance characteristics of a differential scanning calorimeter (DSC) is the instrument baseline, which is the residual heat flow signal of the DSC when operated empty. The DSC is a twin instrument, comprising a sample and a reference calorimeter within a common thermal enclosure, where the two calorimeters are assumed to be identical. The output of the DSC is the difference between the heat flows measured by each of the calorimeters. A number of advantages are gained by the use of twin calorimeters including cancellation of heat leakage and temperature disturbances common to both calorimeters [1]. It follows that if the two calorimeters are identical and symmetrically positioned within the DSC enclosure, the differential heat flow signal of the empty DSC should be zero. However, all DSCs, whether heat flux or power compensation give non-zero heat flow measurements when operated empty, demonstrating that the instrument is not symmetrical. Heat flux DSCs typically have superior baseline when compared to power compensation DSCs, owing to the much smaller temperature differences between the enclosure and the calorimeters in heat flux DSC. Instrument asymmetry and baseline curvature contribute to errors in heat capacity measurements in DSC [2] and MDSC [3].

It is well known that the heat flow signal from a DSC during a transition is an inexact representation of

* Corresponding author. Fax: +1-302-427-4081.
E-mail address: rdanley@tainst.com (R.L. Danley).

[1] Patents applied for

0040-6031/02/$ – see front matter
PII: S0040-6031(02)00212-5

the actual sample heat flow. The measured heat flow is delayed and distorted in time [4]. This distortion or ‘‘smearing’’ of the heat flow signal is the result of the heat capacity of the sample pans and the sensor. These heat capacity effects are present in all DSCs, heat flux or power compensation. Heat storage within a thermal system is analogous to capacitance within an electrical circuit, so that the heat capacity of the sample pan and the sensor effectively filter the measured heat flow. For many DSC experiments, the smeared heat flow is a sufficiently accurate measurement, e.g. when heat flow is integrated over a baseline to obtain the enthalpy of a transition. However, in experiments where partial area integrations are required, e.g. kinetics and purity, the heat flow signal must be de-smeared [5]. The DSC resolution, i.e. the ability to separate closely spaced transitions is improved when the heat capacity effects of pan and sensor are removed from the heat flow signal.

Two de-smearing methods, modeling and numerical deconvolution have generally been used. The modeling approach seeks to represent the DSC by differential equations where the measured signal, which is the differential temperature and it’s derivatives are the inputs and the coefficients of the equations represent the thermal characteristics of the DSC. De-smearing using first and second order differential equations has been demonstrated [6,7]. A difficulty in practicing these methods is the determination of appropriate values for the instrument coefficients [5]. Numerical deconvolution seeks to reconstruct the sample heat flow by employing the convolution integral equation and the apparatus function, which is determined by the response to an impulsive heat input [4]. Numerical deconvolution increases noise in the heat flow signal and is usually only performed after the measurement is complete [5].

2. DSC heat flow measurement theory

In virtually in all DSCs, the measured signal is the difference between the temperatures of the sample and reference positions of the sensor. Within the instrument the ΔT signal is converted to a heat flow rate using a temperature dependent proportionality factor:

$$\dot{q} = E(T)\Delta T \tag{1}$$

the proportionality factor $E(T)$ depends upon the geometry and materials of construction of the differential

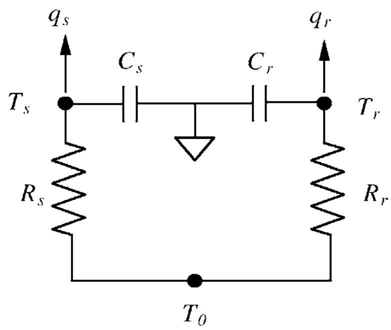

Fig. 1. DSC heat flow measurement model.

temperature sensor. In commercial instruments, the heat flow proportionality factor is generally determined by the manufacturer and is assumed to be the same for all instruments of a given type.

To determine the relationship between the measured temperatures and heat flow, a mathematical model of the measurement apparatus is used. Analysis of the heat flow measurement is based on the lumped heat capacity method where a thermal system is represented by thermal resistances and heat capacities [8]. This type of analysis has frequently been used to model DSCs [9–11]. Fig. 1 shows an equivalent circuit that may be used to represent the heat flow measurement in a DSC. Each calorimeter consists of a thermal resistance and a heat capacity. Subscripts s and r indicate the sample or reference calorimeter. T_s and T_r are the measured temperatures of the sample and reference calorimeters and T_0 is the temperature of the DSC enclosure. The measured heat flows are q_s, the heat flow to the sample and it’s pan and q_r, the heat flow to the reference and it’s pan. This model does not include the sample, reference or their pans.

Performing a heat balance gives the sample and reference heat flows in terms of temperatures T_s, T_r, T_0 and sensor thermal parameters R_s, C_s, R_r, C_r:

$$\dot{q}_s = \frac{T_0 - T_s}{R_s} - C_s \frac{dT_s}{dt} \tag{2}$$

$$\dot{q}_r = \frac{T_0 - T_r}{R_r} - C_r \frac{dT_r}{dt} \tag{3}$$

The difference is taken between the sample and reference heat flows and two differential temperatures are substituted:

$$\Delta T = T_s - T_r; \qquad \Delta T_0 = T_0 - T_s$$

After rearrangement, the result is a four-term heat flow equation giving the difference between the sample and reference heat flows:

$$\dot{q} = -\frac{\Delta T}{R_r} + \Delta T_0\left(\frac{1}{R_s} - \frac{1}{R_r}\right) + (C_r - C_s)\frac{dT_s}{dt} - C_r\frac{d\Delta T}{dt}$$

The first term is equivalent to Eq. (1), the conventional DSC heat flow. The second and third terms reflect imbalances between thermal resistances and heat capacities of the sample and reference calorimeters. The fourth term is a heat flow resulting from differences in heating rate between the sample and reference calorimeters. It is generally zero except when a transition is occurring in the sample, or during modulated DSC (MDSC®) experiments. A principle difference between this heat flow equation and those previously used in DSC is that the calorimeters have not been assumed to be identical. To use this equation, the sensor heat capacities and thermal resistances must be known, the DSC must include the two differential temperature measurements and the sample and reference calorimeters must be independent. A new heat flux DSC and sensor was designed to meet these measurement requirements [12]. A calibration procedure allows the sensor thermal parameters to be determined.

3. DSC heat flux sensor

The twin calorimeter sensor assembly is shown in Fig. 2. It includes provisions for measuring temperatures T_s, T_0 and differential temperatures ΔT and ΔT_0. It is designed such that the sample and reference calorimeters are thermally independent. In other words, heat flow in one calorimeter does not affect the temperature of the other. The main body of the sensor is constantan and consists of a thick flat base and a pair of thin wall closed end cylinders integral with the base. The thin wall section creates the thermal resistance and the flat end surfaces hold the sample and reference. A thin chromel disk is welded to the underside of each platform and functions as an area thermocouple junction to reduce sensitivity to variations of contact between sensor and pans [13]. A chromel wire is welded to each chromel disk. A constantan and a chromel wire are welded to the center of the base structure. The base surface is brazed to the silver DSC enclosure, which makes the base of the sensor assembly isothermal. Differential temperature ΔT is measured between the chromel wires attached to the chromel disks and ΔT_0 is measured between the chromel wires attached to the sample chromel disk and the sensor base. T_s is measured between the sample chromel wire and the base constantan wire. T_0 is measured between the constantan

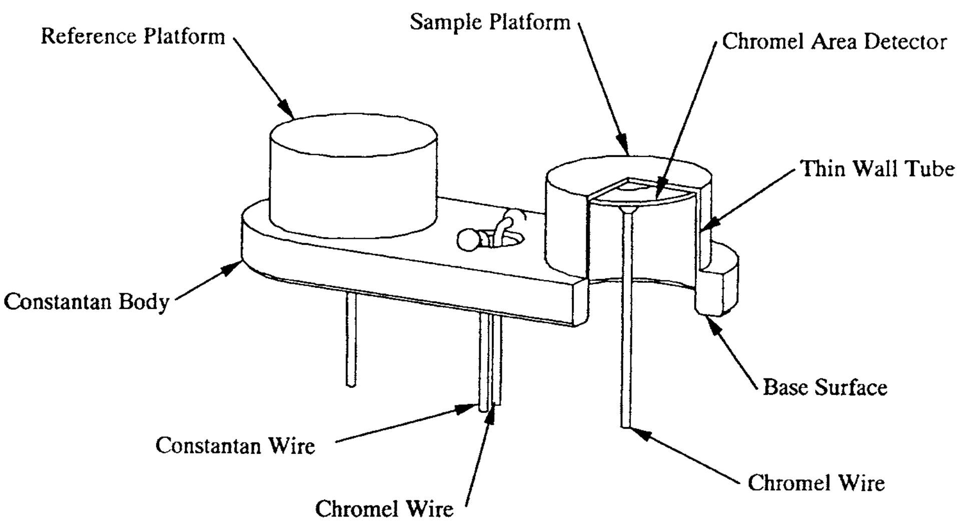

Fig. 2. Tzero™ DSC sensor assembly.

and chromel wires attached to the sensor base. It is used to control the temperature of the DSC.

4. Calibration

Calibration involves the determination of the values for R_s, R_r, C_s and C_r. The calibration procedure includes two identical constant heating rate experiments. The first is performed with the DSC empty and the second with sapphire disks without pans on the sample and reference positions. For the empty DSC experiment, the sample and reference heat flow are set equal to zero, the heat balance Eqs. (2) and (3) are solved, thus giving the calorimeter time constants:

$$\tau_s = C_s R_s = \frac{\Delta T_0}{\mathrm{d}T_s/\mathrm{d}t};$$
$$\tau_r = C_r R_r = \frac{\Delta T_0 - \Delta T}{(\mathrm{d}T_s/\mathrm{d}t) - (\mathrm{d}\Delta T/\mathrm{d}t)}$$

The time constants are a function of temperature. For the sapphire disk experiment, the sample and reference heat flows from Eqs. (2) and (3) are set equal to the heat flow to the sapphire disks, which equals the product of sapphire mass, heat capacity and heating rate. The sample and reference sapphire disk heating rates are assumed to be equal to the heating rates of the sample and reference calorimeters. This is a reasonable assumption, as sapphire has no first order transitions in this temperature region. These equations are solved to give the calorimeter heat capacities:

$$C_s = \frac{m_s c_{\mathrm{sapph}}}{(\Delta T_0/((\mathrm{d}T_s/\mathrm{d}t)\tau_s)) - 1};$$
$$C_r = \frac{m_r c_{\mathrm{sapph}}}{((\Delta T_0 + \Delta T)/((\mathrm{d}T_s/\mathrm{d}t) - (\mathrm{d}\Delta T/\mathrm{d}t)\tau_r)) - 1}$$

where, the calorimeter time constants were determined by the first experiment. Thermal resistances are found using the time constants and heat capacities:

$$R_s = \frac{\tau_s}{C_s}; \qquad R_r = \frac{\tau_r}{C_r}$$

Thus, thermal parameters of the calorimeters as a function of temperature are determined. By contrast with Eq. (1) where a common heat flow calibration curve is applied to all instruments, this procedure results in a unique heat flow calibration for each DSC cell that includes it's unique characteristics.

5. Pan heat capacity effects

The four-term DSC heat flow rate equation above accounts for the sensor heat capacity in the fourth term. However, there is a similar heat flow associated with differences between the sample and reference pan heating rates during transitions or during MDSC. Using the unique capabitities of the new measurement technique, the effects of differences in pan heating rates may be included in the heat flow rate measurement. Fig. 3 shows an electrical network that is analogous to heat flow within the DSC. The model is divided into two parts, the portion below the broken line considered above (labeled sensor) represents the DSC while the portion above the line represents the sample and pans. The measured heat flows are q_s, the heat flow to the sample and it's pan and q_r, the heat flow to the reference and it's pan. The actual sample heat flow is q_{sam}. A heat capacity C_{ps} and a thermal resistance R_p represent the sample pan and the thermal resistance between pan and sensor. The reference pan is assumed to be empty, a heat capacity C_{pr} and a thermal resistance R_p represent the reference pan and the thermal contact resistance between pan and sensor. The sample and reference pan temperatures are T_{ps} and T_{pr}.

Substitute the two measured differential temperatures:

$$\Delta T = T_s - T_r; \qquad \Delta T_0 = T_0 - T_s$$

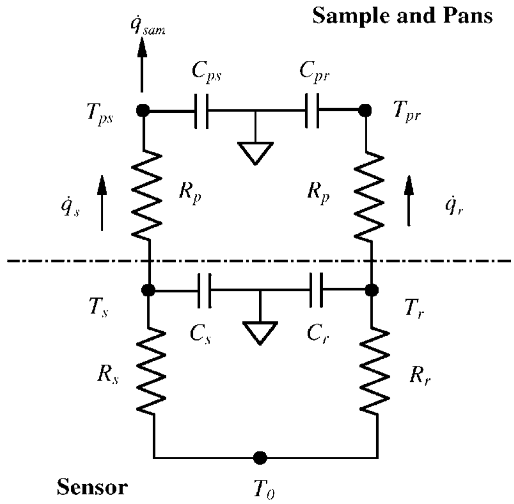

Fig. 3. DSC heat flow measurement model.

into the sample and reference heat flow Eqs. (2) and (3) to obtain the sample and reference heat flow measurement equations:

$$\dot{q}_{\mathrm{s}} = \frac{\Delta T_0}{R_{\mathrm{s}}} - C_{\mathrm{s}}\frac{\mathrm{d}T_{\mathrm{s}}}{\mathrm{d}t};$$

$$\dot{q}_{\mathrm{r}} = \frac{\Delta T_0 + \Delta T}{R_{\mathrm{r}}} - C_{\mathrm{r}}\left(\frac{\mathrm{d}T_{\mathrm{s}}}{\mathrm{d}t} - \frac{\mathrm{d}\Delta T}{\mathrm{d}t}\right)$$

Thermal resistances and heat capacities are obtained using the two part calibration method described above. The measured sample heat flow includes the sample and pan heat flow, likewise the measured reference heat flow is the sum of the pan and reference heat flows.

The objective of the measurement is to recover the actual sample heat flow q_{sam}. The measured sample heat flow is the sum of the sample and sample pan heat flows:

$$\dot{q}_{\mathrm{s}} = \dot{q}_{\mathrm{sam}} + m_{\mathrm{ps}}c_{\mathrm{pan}}\frac{\mathrm{d}T_{\mathrm{ps}}}{\mathrm{d}t}$$

m_{ps} is the sample pan mass, c_{pan} is the specific heat capacity of the pan material. The measured reference heat flow is just the pan heat flow because the reference pan was assumed to be empty:

$$\dot{q}_{\mathrm{r}} = m_{\mathrm{pr}}c_{\mathrm{pan}}\frac{\mathrm{d}T_{\mathrm{pr}}}{\mathrm{d}t}$$

m_{pr} is the reference pan mass. Use the reference heat flow equation to eliminate the pan specific heat capacity and solve for q_{sam}, giving:

$$\dot{q}_{\mathrm{sam}} = \dot{q}_{\mathrm{s}} - \dot{q}_{\mathrm{r}}\left(\frac{m_{\mathrm{ps}}(\mathrm{d}T_{\mathrm{ps}}/\mathrm{d}t)}{m_{\mathrm{pr}}(\mathrm{d}T_{\mathrm{pr}}/\mathrm{d}t)}\right)$$

This equation gives the actual sample heat flow and accounts for pan mass imbalances and heating rate differences between the sample and reference pans. The heat flow measurement equations include imbalances and differences in heating rate between the sample and reference calorimeters. Conventional DSC heat flow measurements using Eq. (1) do not include the sensor imbalances or the differences in heating rate between the sample and reference calorimeters and pans. The heating rate ratio accounts for the fact that during a DSC experiment the heating rates of the sample and reference pans may be different, e.g. during a transition. In conventional DSC, the heat flow measurement is in error because the reference pan does not always heat at the same rate as the sample pan. When the heating rate of the sample pan is higher or lower than the programmed heating rate, the reference heat flow off-setting the sample pan heat flow is too low or too high. The same comments apply to the sensor heat flow. The heat capacity terms in the heat flow measurement equations account for differences between the sample and reference sensor heating rates.

To use this heat flow measurement method, the sample and reference pan temperatures are needed. They are not measured directly but may be obtained from the measured quantities. Heat flow between the sample and reference pans and their sensors are given by:

$$\dot{q}_{\mathrm{s}} = \frac{T_{\mathrm{s}} - T_{\mathrm{ps}}}{R_{\mathrm{p}}}; \qquad \dot{q}_{\mathrm{r}} = \frac{T_{\mathrm{r}} - T_{\mathrm{pr}}}{R_{\mathrm{p}}}$$

which are solved to find the pan temperatures:

$$T_{\mathrm{ps}} = T_{\mathrm{s}} - \dot{q}_{\mathrm{s}}R_{\mathrm{p}}; \qquad T_{\mathrm{pr}} = T_{\mathrm{r}} - \dot{q}_{\mathrm{r}}R_{\mathrm{p}}$$

Sensor temperatures and heat flows are measured, the pan contact resistance R_{p} is needed to determine the pan temperatures. When the temperature differences between two surfaces in contact is small, as in the case of the DSC pan, the heat exchange between the surfaces consists of parallel heat conduction through the solid surfaces in contact and through the gas in the interstices [14]. A model equation is used to calculate the contact resistance between the pan and sensor. It assumes that there are two parallel heat conduction paths between the pan and the sensor. One is solid conduction through the sensor and pan where they contact one another and the other is conduction through the gas layer between the pan and sensor. The solid conduction path consists of pan and sensor thermal resistances in series. The equation used for the contact resistance is:

$$R_{\mathrm{p}} = \frac{1}{(1/(R_{\mathrm{pan}} + R_{\mathrm{sen}})) + (1/R_{\mathrm{gas}})}$$

where subscripts pan, sen and gas indicate thermal resistances associated with the pan, the sensor and the purge gas. The component thermal resistances are calculated from:

$$R = \frac{1}{\alpha k}$$

where k is the thermal conductivity of the pan, sensor or purge gas and α is a geometric factor for the pan, sensor or purge gas that is equivalent to the ratio of an area to a length. Thermal conductivities for each component as a function of temperature are known, the geometric factors have been determined from a multivariate curve fit of experimental data. The geometric factors are dependent upon the pan and sensor shape. Typical values of the geometric factors are supplied in the instrument software for selected pan types. These capabilities are incorporated in the TA Instruments Q1000™ DSC [12].

6. Experimental

All experiments were performed using a TA Instruments Q1000™ DSC with a refrigerated cooling system (RCS) installed. The DSC incorporates the heat flow sensor assembly and heat flow measurement methods. Calibration of the sensor parameters was performed using the RCS at a heating rate of 20 °C/min. The DSC cell and the RCS were purged with nitrogen. Baselines were run at 20 °C/min. using the RCS. Crimped aluminum pans were used with 5.64 mg indium and 1.13 mg dotriacontaine samples.

7. Results and discussion

A comparison of the empty DSC baseline of a Q1000™ with RCS and a 2920 DSC with RCS is shown in Fig. 4. This comparison is particularly apt, because the 2920 is notable for it's excellent baseline performance. The Q1000™ baseline is superior in every way, the start-up offset is much smaller, the baseline is dramatically straighter and slope is greatly reduced. As expected of a twin calorimeter, the empty instrument heat flow signal is very nearly zero throughout the experiment. Notice that the heat flow scale is 1.0 mW and that the Q1000™ data extends from −80 to 400 °C.

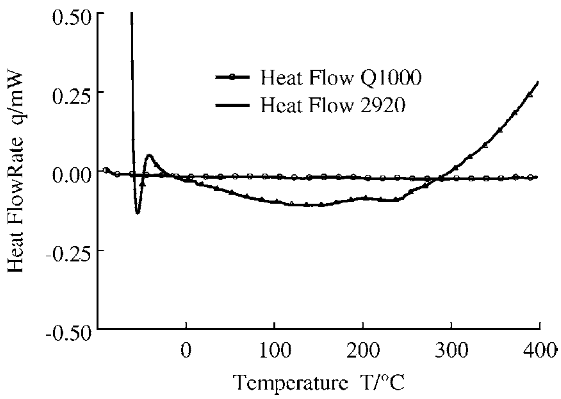

Fig. 4. DSC baseline comparison.

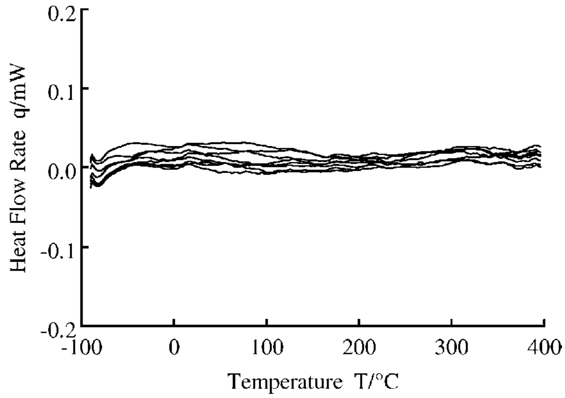

Fig. 5. Q1000™ instrument baselines using RCS.

Fig. 5 shows a plot of instrument baselines produced by the Q1000™ DSC using the RCS. Eight consecutive scans were made between −90 and 400 °C to demonstrate baseline performance. The total range of heat flow variation is less than 40 μW. All baselines are very straight, have very little slope and very small start-up offsets. Between any two consecutive baselines the variation is no greater than 20 μW. These results show that excellent baseline performance may be obtained over a very broad range of temperatures with excellent repeatability. Among the benefits of the baseline improvements achieved by the Tzero™ DSC are the ability to measure very weak transitions [15].

Fig. 6 shows an indium melt at 20 °C/min. Two heat flows are plotted, the conventional DSC heat flow and the heat flow according to the Advanced Tzero™ heat flow measurement of this paper. The conventional DSC heat flow signal is calculated using Eq. (1). Comparing the Advanced Tzero™ heat flow to the conventional heat flow, the peak height increased from 23.2 to 29.9 mW and the peak width at half height has decreased dramatically from 2.26 to 0.82 °C, nearly a three-fold reduction in peak width. The onset and peak temperatures are slightly lower due to the elimination of thermal lag of the sample calorimeter and sample pan. The baseline return at the completion of the melt

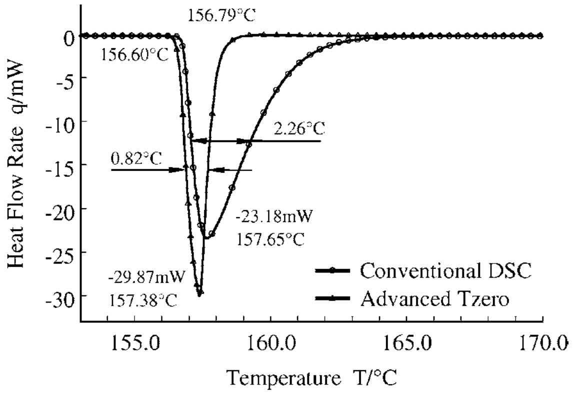

Fig. 6. Indium melt Tzero™ vs. conventional DSC.

is much faster, corresponding to improved dynamic response that yields better resolution.

Fig. 7 shows the result of a 10 °C/min DSC experiment with a 1.13 mg sample of dotriacontane, a C32 hydrocarbon. Two heat flow signals are shown, Advanced Tzero™ and conventional DSC. This sample has three closely spaced transitions demonstrating the separation ability of a DSC (i.e. the resolution). The first two transitions are barely separated from one another by conventional DSC, whereas Advanced Tzero™ shows a substantial improvement in the separation. However, between the second and third transitions, Advanced Tzero™ clearly reaches baseline, where conventional DSC does not. In this case, the ability to accurately determine the enthalpy of the third transition is improved by Advanced Tzero™ as compared to conventional DSC. All peak heights are substantially increased while peak width is

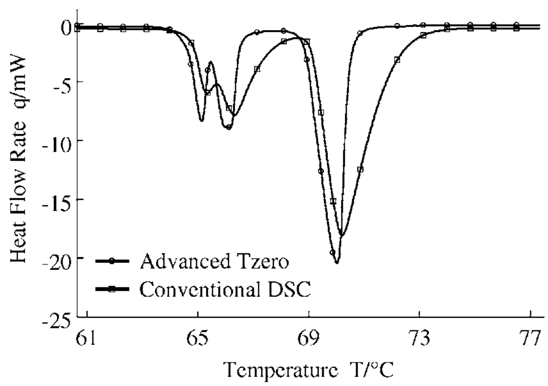

Fig. 7. 1.13 mg dotriacontane at 10 °C/min.

considerably reduced. Analysis of additional experiments confirms the improved resolution [16].

8. Conclusions

Beginning from first principles, a new DSC heat flow measurement technique has been developed. It includes three principal components, a new sensor assembly, more comprehensive heat flow measurement equations and a novel heat flow calibration method. The new sensor assembly incorporates independent sample and reference calorimeters and uses two differential temperature measurements. Unlike traditional DSC, the measurement equations do not include the assumption that the instrument is perfectly symmetric, thus the measurement includes the effects of sensor asymmetry. The measurement also includes the effects of differences between the sample and reference calorimeter heating rates and the sample and reference pan heating rates. The calibration technique gives a more thorough characterization of the DSC sensor and includes the effects of asymmetry. The calibration procedure also provides a unique heat flow calibration for each instrument, incorporating it's characteristics as opposed to the use of a generic heat flow calibration function common in other DSCs.

The experimental results show the benefits of these improvements, which include a dramatic improvement in the instrument baseline and improvements in resolution. Improvements in the instrument baseline benefit nearly all DSC experiments, but are especially important for heat capacity measurements and for detection and quantification of weak and broad transitions. Enhancements in resolution improve the ability to unambiguously separate and quantify closely spaced transitions. Partial area integrations will be improved by the rapid return to baseline at the completion of a transition.

References

[1] W. Hemminger, G. Höhne, Calorimetry Fundamentals and Practice, Verlag, Weinheim, 1984, pp. 77–79.

[2] V.B.F. Mathot, in: V.B.F. Mathot (Ed.), Calorimetry and Thermal Analysis of Polymers, Hanser/Gardner, Cincinnati, 1994, pp. 108–109.

[3] A. Boller et al., J. Therm. Anal. 49 (1997) 1081.
[4] G.W.H. Höhne, Thermochim. Acta 22 (1978) 347.
[5] G.W.H. Höhne, W. Hemminger, H.-J. Flammersheim, Differential Scanning Calorimetry, Springer, Berlin, 1996, pp. 89–96.
[6] K.H. Schönborn, Thermochim. Acta 69 (1983) 103.
[7] K.-R. Löblich, Thermochim. Acta 85 (1985) 263.
[8] J.P. Holman, Heat Transfer, McGraw-Hill, New York, 4th Edition, 1976, pp. 97–102.
[9] A.P. Gray, in: R.S. Porter, J.F. Johnson (Eds.), Analytical Calorimetry, Vol. 1, Plenum Press, New York, 1968, pp. 209–218.
[10] R.A. Baxter, in: R.F. Schwenker, P.D. Garn (Eds.), Thermal Analysis, Vol. 1, Academic Press, New York, 1969, pp. 65–84.
[11] G.W.H. Höhne, W. Hemminger, H.-J. Flammersheim, Differential Scanning Calorimetry, Springer, Berlin, 1996, pp. 21–33.
[12] L. Waguespack, R.L. Blaine, in: Proceedings of the 29th Conference of North American Thermal Analytical Society, 2001, pp. 721–727.
[13] US Patent 4,095,453, Differential Thermal Analysis Cell, 1978.
[14] C.V. Madhusudana, Thermal Contact Conductance, Springer, New York, 1996, pp 1–3.
[15] P.A. Caulfield, L.C. Thomas, in: Proceedings of the 29th Conference of North American Thermal Analytical Society, 2001, pp. 798–803.
[16] P.A. Caulfield, R.L. Danley, in: Proceedings of the 29th Conference of North American Thermal Analytical Society, 2001, pp. 735–740.